Surface Reconstruction with a Fractional Hole: $(\sqrt{5} \times \sqrt{5})R26.6°$ $LaAlO_3$ (001)

C. H. Lanier,[1] J. M. Rondinelli,[1,*] B. Deng,[1] R. Kilaas,[1] K. R. Poeppelmeier,[2] and L. D. Marks[1,†]

[1]*Department of Materials Science and Engineering, Northwestern University, Evanston, Illinois 60208, USA*

[2]*Department of Chemistry, Northwestern University, Evanston, Illinois 60208, USA*

(Received 7 November 2006; published 21 February 2007)

The structure of the $(\sqrt{5} \times \sqrt{5})R26.6°$ reconstruction of $LaAlO_3$ (001) has been determined using transmission electron diffraction combined with direct methods. It has a lanthanum oxide termination with one lanthanum vacancy per surface unit cell. Density functional calculations indicate that charge compensation occurs by a fractional number of highly delocalized holes, and that the surface contains no oxygen vacancies and the holes are not filled with hydrogen. The reconstruction can be understood in terms of expulsion of the more electropositive cation from the surface and increased covalency.

DOI: 10.1103/PhysRevLett.98.086102 PACS numbers: 68.35.Bs, 61.14.Lj, 68.37.Lp, 73.25.+i

Lanthanum aluminate ($LaAlO_3$, LAO) is an important oxide material as a substrate for thin film growth [1–4], a potential gate dielectric (or buffer layer) [5–11], as well as a catalyst [12–14]. This transition metal oxide is representative of a larger class of materials with ABO_3 stoichiometry known as perovskites. There has recently been interest in the character of the interfaces between $LaAlO_3$ (001) and other materials such as Si and $SrTiO_3$ [15,16]. Since both La and Al are almost always in a trivalent state, conventional methods of counting carriers for charge compensation lead to the unusual conclusion that a fractional number of excess carriers per unit cell is required.

$LaAlO_3$ (001) consists of alternating layers of LaO and AlO_2 stacked along the $\langle 001 \rangle$ cubic direction. Consequently, the formal charges of La^{3+}, Al^{3+}, and O^{2-} produce two terminations differing in nominal charges of $(La\text{-}O)^{+}$ and $(Al\text{-}O_2)^{-}$, and an excess half electron (or hole) exists per unit interface cell. The LAO (001) surface is therefore polar and classified as a Type III surface within Tasker's convention [17]. The composition, structure and morphology of LAO (001) has been researched in the past few years; however, structural information of how the surface terminates is still ambiguous. The majority of the analyses [4,18–24] have considered a (1×1) surface prepared by relatively low-temperature annealing (the melting point of $LaAlO_3$ is 2110 °C) in various atmospheres, and report either (or both) LaO and AlO_2 terminations; it is not clear whether the surfaces have reached thermodynamic equilibrium. The only reported reconstructions on the (001) surface of LAO is a (5×5) reconstruction obtained by annealing at 1500 °C for 20 h in air [25]. Furthermore, very little of the work has addressed the issue of charge compensation and how to reconcile the dipole at the surface. In this Letter, we report experimental results for the $(\sqrt{5} \times \sqrt{5})R26.6°$ surface reconstruction, hereafter referred to as RT5, on the $LaAlO_3$ (001) surface. We also provide a first-principles investigation of the structure and show how the polar surface is passivated through a redistribution of the near surface electron density.

Single crystal $LaAlO_3$ (001) wafers from the MTI Corporation (99.95% pure) were prepared for transmission electron microscopy studies using conventional methods of dimpling and ion-beam thinning (using a Gatan Precision Ion Polishing System with 4.8 kV Ar^{+} ions) until electron transparent. They were then annealed at temperatures between 1100–1500 °C in a Carbolite STF 15/51/180 tube furnace for 3 h. While initial experiments were performed in air, we also annealed in a mix of 20% O_2: 80% N_2, which mass-spectrometer measurements indicated had a maximum impurity level of 10 ppb of H_2O.

Diffraction experiments were performed with a Hitachi 8100 electron microscope operating at 200 kV. Negatives with exposure times ranging from 0.5 to 90 s were recorded then and digitized to 8 bits with a 25 μm pixel size on an Optronics P-1000 microdensitometer which was calibrated to be linear over the selected exposure range. Intensity measurements were determined using a cross-correlation technique [26], and the data sets (7911 surface reflections) were symmetry reduced using $p4$ plane group symmetry to 94 independent beams with the error for each reflection determined using robust statistical methods. These were analyzed using electron direct methods (EDM 2.0.1) software [27] and in-plane atomic positions refined against the experimental data gave a $\chi^2 = 4.83$.

For the theoretical modeling, the LAO surface structure was geometry optimized using a three-dimensional periodic density-functional theory (DFT) surface slab model of 9 layers (118 atoms) separated by 8 Å of vacuum. To analyze the charge density, calculations were performed using the all-electron (linearized) augmented-plane wave + local orbitals (L/APW + lo) method as implemented in WIEN2K [28] with the Perdew-Wang (PW96)-generalized gradient approximation [29] exchange-correlation functional, a plane-wave cutoff of $RK_{\max} = 6.75$ and muffin-tin radii of 1.75, 1.75, and 2.33 Bohr for O, Al, and La, respectively. To test for water splitting and oxygen vacancies, calculations were also performed using the projector augmented wave (PAW) approach [30] as implemented in the Vienna *ab initio* simulation package (VASP) code [31,32] using a $3 \times 3 \times 1$ k-point grid, plane-wave energy cutoff of 360 eV, electronic iteration conver-

gence of 0.001 eV, and geometry relaxation convergence of 0.01 eV. The Fermi surface was smeared using a Gaussian width of 0.20 eV, and the conventional local-density approximation (LDA) as well as the Perdew, Burke, Ernzerhof (PBE) [33] and PW92 [34] functionals were used with DFT minimized lattice parameters.

A typical transmission electron diffraction pattern of the reconstructed surface is shown in Fig. 1. The surface is well ordered with facets evident in the dark field image and minimal diffuse background scattering from disorder present in the diffraction pattern (inset). Direct methods analysis and refinement were straightforward, and gave the structure shown in Fig. 2; information about the atomic positions can be found in Table I, while the experimental and calculated intensities are given in Ref. [35].

Bulk LAO has a rhombohedral to cubic phase transition at $435 \pm 25\,^{\circ}\mathrm{C}$. Consequently, the RT5 reconstruction forms on a cubic LAO substrate, but this substrate becomes rhombohedral upon cooling. As the structures of rhombohedral LAO and cubic LAO only differ by tenths of a degree, it is reasonable to expect the cubic surface reconstruction to be accommodated on bulk rhombohedral LAO at room temperature. Nonetheless, both a rhombohedral and a cubic surface structure were explored and a $p4$ symmetry provided the best fit to the data. The possibility of an aluminum overlayer was also considered; however, the fit to the data was noticeably inferior.

The RT5 reconstruction is an overlayer of lanthanum oxide on the AlO_2 bulk termination of LAO with one La vacancy per surface unit cell. The surface stoichiometry may be written as $(V\mathrm{La}_4\mathrm{O}_5)^{-1/2}$, where V is the lanthanum cation vacancy and the surface unit has a nominal charge of $-\frac{1}{2}$. Each surface lanthanum (La1) is coordinated to four oxygens within the surface layer and four oxygens in the layer below. Additionally, the lanthanum atom is displaced into the bulk by ≈ 0.20 Å, while the oxygen atoms are displaced away from the bulk. The surface layer oxygen atoms (O1 and O2) preserve the octahedral coordination of the Al atoms in the layer below; however due to the La vacancy, O1 is now only four-coordinate while O2 is five-coordinate.

The formation of the RT5 reconstruction can be understood as follows. To reduce positive charge on the surface of an ideal LaO bulk termination, either La^{3+} or Al^{3+} cation vacancies are formed. Because La^{3+} is less electronegative than Al^{3+}, lanthanum vacancies are favored. It follows that the surface bond covalency should increase to satisfy the under coordination of the surface oxygens. Therefore, since the La-O bonds are longer compared to the Al-O bonds, and the nonbonding oxygen repulsive interactions are smaller than those of the Al-O octahedra, the La-O bonds become shorter, with an average La-O bond length of 2.61 Å (compared to 2.68 Å in the bulk). Despite these significant changes, a persistent, albeit reduced, polarization remains at the surface.

The lanthanum cation expulsion nearly reconciles the charge neutrality problem at the surface. For the RT5 reconstruction with an area equal to five interface unit cells of the bulk, it is impossible to form a fully charge compensated surface without invoking a fractional density (per reconstructed surface cell) of carriers or a partial occupancy of cation sites. While there was too little diffuse intensity in the diffraction data to support a fractional occupancy of sites, a low density of oxygen vacancies is undetectable experimentally. Similarly, there is the possibility of disordered hydrogen atoms on the surface and several studies indicate that some bulk oxides (and surfaces) can contain low levels of hydrogen [36–40].

To test for the presence of hydrogen on the surface, we considered the possible reaction

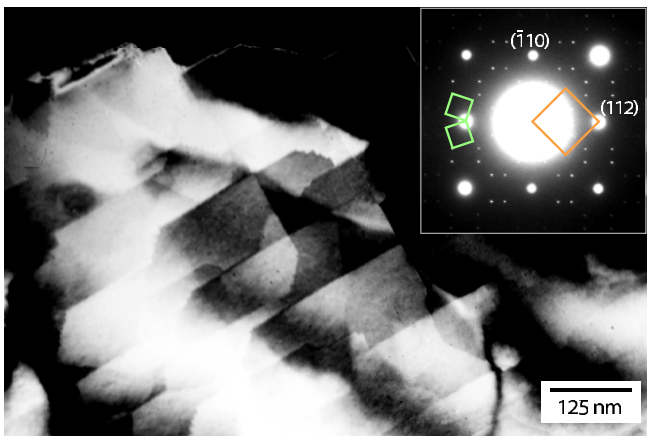

FIG. 1 (color online). Dark field image showing extended ⟨100⟩ faceting with step bunches and reconstructed terraces. A small probe off-zone diffraction pattern (inset) is shown with the rhombohedral (1×1) bulk unit cell (right) and the surface unit cell for both domains of the reconstruction (left).

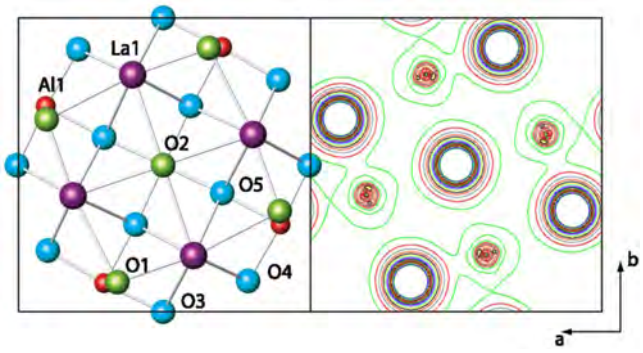

FIG. 2 (color online). Top view of the RT5 surface reconstruction (left) with the surface unit cell outlined in black ($a = 8.537$ Å). Contour map of the valence density in the surface plane (right) at 0.1 $e/\mathrm{Å}^3$ showing the increased electron density between the surface oxygen (O1 and O2) and lanthanum atoms (La1) corresponding to increased covalent bonding. The La vacancy is at the corner of the unit cell; atoms O1, O2, and La1 are in the surface layer, while Al1, O3, O4, and O5 are in the second layer.

TABLE I. Atom positions for the RT5 reconstruction are given as fractional coordinates of the surface cell ($a = 8.526$ Å). The La vacancy is denoted by V at the surface (layer 1) and the bulk corresponds to layer 5. $\Delta_z = |z_{\mathrm{DFT}} - z_{\mathrm{Bulk}}|$ in Å and positive (negative) deviations indicate a displacement away from (into) the bulk. The excess charge values for each atom are denoted by δQ (10^{-2} e), and the integrated hole density as $\rho(h)$ (10^{-2} e/Å^2). Bulk LAO provides the charge reference: O = −1.540 e, La = 2.065 e, and Al = 2.554 e.

		Experiment		WIEN2K					
Layer	Atom	x	y	x	y	z	Δ_z	δQ	$\rho(h)$
1	V	0.00	0.00	0.000	0.000	0.320	⋯	⋯	⋯
	O1	0.34	0.90	0.344	0.898	0.320	+0.036	10.2	2.1
	O2	0.50	0.50	0.500	0.500	0.321	+0.055	5.8	2.5
	La1	0.81	0.40	0.808	0.396	0.310	−0.196	−2.6	0.3
2	Al1	0.30	0.90	0.298	0.901	0.240	+0.035	−0.7	0.0
	Al2	0.50	0.50	0.500	0.500	0.239	+0.015	−0.7	0.0
	O3	0.50	0.00	0.500	0.000	0.232	−0.169	4.1	2.0
	O4	0.21	0.11	0.210	0.106	0.239	+0.009	1.4	0.6
	O5	0.70	0.59	0.702	0.594	0.237	−0.041	2.0	1.3
3	O6	0.29	0.90	0.290	0.899	0.159	−0.007	2.0	1.8
	O7	0.50	0.50	0.500	0.500	0.158	−0.018	2.2	2.5
	La2	0.80	0.40	0.800	0.399	0.158	−0.036	−0.3	0.2
	La3	0.00	0.00	0.000	0.000	0.163	+0.099	1.9	0.2
4	Al3	0.30	0.90	0.298	0.900	0.079	−0.003	0.0	0.0
	Al4	0.50	0.50	0.500	0.500	0.079	−0.008	0.3	0.0
	O8	0.50	0.00	0.500	0.000	0.081	+0.038	0.7	0.7
	O9	0.20	0.10	0.201	0.100	0.078	−0.045	0.4	1.3
	O10	0.70	0.60	0.700	0.600	0.079	−0.009	0.5	1.0
5	O11	0.29	0.90	0.304	0.900	0.000	n/a	1.3	1.9
	O12	0.50	0.50	0.500	0.500	0.000	n/a	0.4	1.0
	La4	0.80	0.40	0.800	0.400	0.000	n/a	−0.2	0.2
	La5	0.00	0.00	0.000	0.000	0.000	n/a	0.3	0.2

$$4(\mathrm{RT5}) + H_2O \rightleftharpoons 4(\mathrm{RT5H}_{1/2}) + \tfrac{1}{2}O_2$$

with partial occupancy of a hydrogen bonded to O1 (lower in energy than the alternative O2). Four calculations were performed using VASP: one without hydrogen for a $\sqrt{10} \times \sqrt{10}$ supercell (9 layers, 236 atoms) rotated by 45° containing two surfaces each with four RT5 unit cells, another of the same cell but with $\frac{1}{2}$ hydrogen per RT5 surface unit cell (atomic positions are given in Ref. [35]) and two for the isolated molecules H_2O and O_2. The DFT calculations indicated that this reaction can occur with an energy change of −0.99 eV at $T = 0$ K for the PBE functional, −1.04 eV with the PW92 functional and −1.46 eV for the LDA. By comparing the PBE and PW92 numbers we can estimate that the intrinsic surface uncertainty [41] is small, about 0.15 eV. A reasonable estimate of the error in the energies is $|E_{\mathrm{LDA}} - E_{\mathrm{PBE}}|/2$, or 0.24 eV. Thus, at a 99% confidence level (3σ) the maximum energy for this exothermic reaction would be −1.71 eV at $T = 0$ K. Using tabulated values for the free-energy of water and oxygen [42] the reaction becomes endothermic and would require more than 3.64 eV to take place at the RT5 formation temperature of 1200 °C in an air atmosphere with less than 10 ppb water impurity. Hence, to a better than 99% confidence level when the reconstruction is formed at high temperature, it is energetically unfavorable for the surface to split water and incorporate H^+. On cooling and exposure to environmental humidity it is quite possible that the surface splits water [43].

Similarly, to test for the presence of oxygen vacancies on the RT5 surface, we considered two reduced structures with a $\frac{1}{4}$ oxygen vacancy per unit cell at sites O1 and O2 (the structures are available in Ref. [35]). It was found that at $T = 0$ K the lower energy reduced structure (vacancy at O1) is 2.58 eV higher in energy than the RT5 structure as presented. At the reconstruction formation temperature, the oxygen chemical potential is large enough to reduce the surface with an energy gain of −0.29 eV; however, within the error associated with these computational methods, we posit the probability for this reduction is small. Furthermore, as the sample is cooled the oxygen vacancies (if any) would be filled and the RT5 surface is preserved. Again, we find that an alternative charge compensation mechanism is required, and suggest that an electron hole fulfills this requirement.

Hole densities were calculated by integrating over the Bader volumes [44]. Somewhat unusual is that the hole densities do not decay off into the bulk, but rather the fractional hole is very delocalized over all the oxygen atoms, as indicated by the projected hole density of states along the [100] direction normal to the surface shown in Fig. 3. This behavior is atypical for most bulk oxides since hole trapping occurs through acceptor defect sites in open lattice perovskite structures [45]. This effect leads to small hole mobilities in bulk materials, and is reminiscent of the Mott-Wannier exciton model in more ionic crystals (despite the increased covalency here).

Although the charge on the atoms in a solid cannot be uniquely partitioned, there are several theoretical models which allow for its estimation; we used Bader's *atom-in-molecule* method [46] with the WIEN2K densities. Table I includes the excess charges (δQ) calculated for the various layers. There is a noticeable decrease in the charge on the surface oxygen atoms (O1 and O2) as well as the surface lanthanum (La1), with smaller variations decaying off more rapidly into the bulk for the other oxygen atoms. In bulk $LaAlO_3$ the Al-O bond has more covalent character than the La-O bond; the charge densities at the (3, −1)

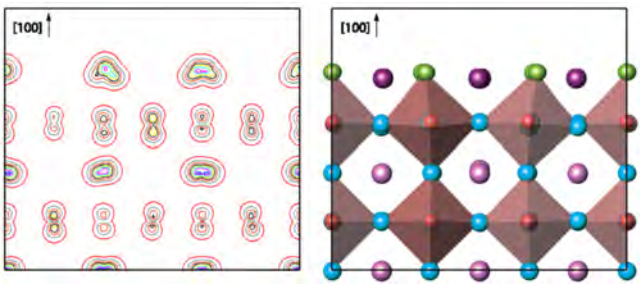

FIG. 3 (color online). Integrated hole density plot along the [100] direction at 0.01 e/Å^2 shown next to the crystal structure.

bond critical points, which are typically used as a qualitative estimate, are ≈ 0.45 and $0.24\ \mathrm{eV}/\mathrm{\AA}^3$ for the two. At the surface there is essentially no change in the covalent character of the Al-O bonds, but the density between the La-O at the surface increases dramatically to a value of $\approx 0.50\ \mathrm{eV}/\mathrm{\AA}^3$ for the closest oxygen atom which is only 2.37 Å away compared to 2.70 Å in the bulk. This suggests that some of the charge on the oxygen ions in the bulk transfers into the covalent bonds near the surface, and rather independent of this, it occurs in the presence of a highly delocalized hole.

For the RT5 reconstruction on the $LaAlO_3$ (001) surface, the surface polarity is quenched by the presence of the electron hole. This point has strong implications on the growth of nanolayer composites and the dynamics describing surface reconstructions, that is, interface passivation is highly sensitive to the experimental preparation. Furthermore, it is likely that oxygen vacancies can strongly influence the formation of charge carriers at such interfaces; while the results suggest that they are filled upon annealing, it is important to recognize that their electron donor character may behave differently at interfaces. We find that the driving force for reconstruction is the polar discontinuity at the surface and charge neutrality requires either (or both) atomic or electronic reconfiguration: the expulsion of the lanthanum cation and delocalized electron hole meets this challenge.

This work was funded by NSF under Grant No. DMR-0455371 (J. M. R.) and by the DOE under Contract No. DE-FG02-01ER45945/A006 (B. D. and R. K.) and DE-FG02-03ER15457 (C. H. L.).

*Present address: Materials Department, University of California, Santa Barbara, CA, 93106-5050, USA.
†Corresponding author.
Electronic address: L-marks@northwestern.edu

[1] R. Brown *et al.*, Appl. Phys. Lett. **57**, 1351 (1990).
[2] H. Schneidewind, M. Manzel, and K. Kirsch, IEEE Trans. Appl. Supercond. **11**, 3106 (2001).
[3] R. W. Simon *et al.*, Appl. Phys. Lett. **53**, 2677 (1988).
[4] D. A. Schmidt *et al.*, J. Appl. Phys. **99**, 113521 (2006).
[5] M. V. Cabanas *et al.*, Solid State Ionics **101**, 191 (1997).
[6] C. J. Forst, K. Schwarz, and P. E. Blochl, Phys. Rev. Lett. **95**, 137602 (2005).
[7] H. Y. Hwang, MRS Bull. **31**, 28 (2006).
[8] D. O. Klenov, D. G. Schlom, H. Li, and S. Stemmer, Jpn. J. Appl. Phys. **44**, L617 (2005).
[9] N. Nakagawa, H. Y. Hwang, and D. A. Muller, Nat. Mater. **5**, 204 (2006).
[10] B.-E. Park and H. Ishiwara, Appl. Phys. Lett. **79**, 806 (2001).
[11] A. Ohtomo and H. Y. Hwang, Nature (London) **427**, 423 (2004).
[12] T. Yamamoto *et al.*, J. Synchrotron Radiat. **8**, 634 (2001).
[13] M. Valden *et al.*, J. Catal. **161**, 614 (1996).
[14] S. Liu *et al.*, Catal. Lett. **63**, 167 (1999).
[15] A. Ohtomo *et al.*, Nature (London) **419**, 378 (2002).
[16] A. A. Knizhnik *et al.*, Phys. Rev. B **72**, 235329 (2005).
[17] P. W. Tasker, J. Phys. C **12**, 4977 (1979).
[18] R. J. Francis, S. C. Moss, and A. J. Jacobson, Phys. Rev. B **64**, 235425 (2001).
[19] J. Yao *et al.*, J. Chem. Phys. **108**, 1645 (1998).
[20] H. Kawanowa *et al.*, Surf. Sci. **506**, 87 (2002).
[21] Z. L. Wang and A. J. Shapiro, Surf. Sci. **328**, 141 (1995).
[22] P. A. W. van der Heide and J. W. Rabalais, Chem. Phys. Lett. **297**, 350 (1998).
[23] J.-P. Jacobs, M. A. S. Miguel, and L. J. Alvarez, THEOCHEM **390**, 193 (1997).
[24] J.-P. Jacobs *et al.*, Surf. Sci. **389**, L1147 (1997).
[25] Z. L. Wang and A. J. Shapiro, Surf. Sci. **328**, 159 (1995).
[26] P. Xu, G. Jayaram, and L. D. Marks, Ultramicroscopy **53**, 15 (1994).
[27] R. Kilaas *et al.*, computer code, EDM: Electron Direct Methods,V.2.0.1 (2006); www.numis.northwestern.edu/edm.
[28] P. Blaha *et al.*, *An Augmented Plane Wave + Local Orbitals Program for Calculating Crystal Properties* (Karlheinz Schwarz, Techn. Universitat Wien, Austria, 2001) ISBN 3-9501031-1-2.
[29] J. P. Perdew, K. Burke, and Y. Wang, Phys. Rev. B **54**, 16 533 (1996).
[30] P. E. Blochl, Phys. Rev. B **50**, 17 953 (1994).
[31] G. Kresse and J. Furthmuller, Phys. Rev. B **54**, 11 169 (1996).
[32] G. Kresse and D. Joubert, Phys. Rev. B **59**, 1758 (1999).
[33] J. P. Perdew, K. Burke, and M. Ernzerhof, Phys. Rev. Lett. **77**, 3865 (1996).
[34] J. P. Perdew and Y. Wang, Phys. Rev. B **45**, 13 244 (1992).
[35] See EPAPS Document No. E-PRLTAO-98-024709 for crystallographic structure information and atom positions used in electronic structure calculations. For more information on EPAPS, see http://www.aip.org/pubservs/epaps.html.
[36] X.-G. Wang, A. Chaka, and M. Scheffler, Phys. Rev. Lett. **84**, 3650 (2000).
[37] V. K. Lazarov *et al.*, Phys. Rev. B **71**, 115434 (2005).
[38] C. Noguera, F. Finocchi, and J. Goniakowski, J. Phys. Condens. Matter **16**, S2509 (2004).
[39] C. Woll, J. Phys. Condens. Matter **16**, S2981 (2004).
[40] C. G. Van de Walle, Phys. Rev. Lett. **85**, 1012 (2000).
[41] A. E. Mattsson, R. Armiento, P. A. Schultz, and T. R. Mattsson, Phys. Rev. B **73**, 195123 (2006).
[42] M. W. Chase, Jr. *et al.*, JANAF Thermochemical Tables [J. Phys. Chem. Ref. Data 14, No. 1 (1985)], 3rd ed.
[43] At STP and saturated H_2O the thermolysis of water requires ≈ 0.50 eV, which is within the error of these DFT calculations.
[44] Calculated by adding an extra half electron per surface unit cell then subtracting the normal density.
[45] H. Donnerberg, S. Többen, and A. Birkholz, J. Phys. Condens. Matter **9**, 6359 (1997).
[46] R. F. W. Bader, *Atoms in Molecules: A Quantum Theory* (Clarendon, Oxford, 1990).